

## Duty Ratio-Controlled Surface Roughness of Silicon Nitride Film deposited using Room-Temperature SiH<sub>4</sub>-NH<sub>3</sub>-N<sub>2</sub> Plasma

Daehyun Kim,<sup>1</sup> Byungwhan Kim,<sup>1,\*</sup> and Yong-Ho Seo<sup>2</sup>

<sup>1</sup>Department of Electronic Engineering, Sejong University, Seoul 143-747, Korea

<sup>2</sup>Nanotechnology and Advanced Materials Engineering, Sejong University, Seoul 143-747, Korea

Silicon nitride films were deposited with mixed gasses of SiH<sub>4</sub>-NH<sub>3</sub>-N<sub>2</sub> using a pulsed, plasma-enhanced chemical vapor deposition system at room temperature. The surface morphology of the SiN films was investigated as a function of the bias power and duty ratio, which varied from 40 W to 100 W and 30% to 90%, respectively. The surface roughness is detailed in terms of the mean surface roughness, nonuniformity of the pixel height distribution, and minimum pixel range. Ion energy diagnostic data is correlated with the surface morphology. An empirical model constructed is used to examine the impact of the ion energy on the surface morphology. As the duty ratio varied under a fixed power level, the lowest degree of surface roughness was obtained at a relatively low duty ratio of 50% at all powers except 100 W. It is not able that this is strongly correlated with the ion energy flux. Additionally, as the power varied at a fixed duty ratio, less surface roughness was noted at a relatively low power of 60 W. With variations in the power, the surface roughness strongly depended on the ion energy. For all variations in the process parameters, the surface roughness varied between 0.285 nm and 2.249 nm. The non-uniformity of the pixel height distribution was lowest at 50% at all powers except 60 W. A neural network model was utilized to explore the parameter effect.

**Keywords:** surface roughness, silicon nitride film, pulsed plasma-enhanced chemical vapor deposition, atom force microscopy, room-temperature, non-uniformity

### 1. INTRODUCTION

In manufacturing electronic devices such as memory or solar cells, silicon nitride (SiN) films are widely used as a dielectric or an anti-reflective layer. As an encapsulation layer for organic light emitting displays, SiN films are also actively adopted. This arises from the good thermal stability, high electrical resistivity, and good chemical inertness of these types of films. Plasma-enhanced chemical vapor deposition (PECVD) is a popular means of depositing SiN films.<sup>[1-8]</sup> A number of promising features of SiN films deposited at room temperature have been reported. These include a high deposition rate with a low radio frequency (RF) source power,<sup>[5]</sup> a high refractive index at a lower bias power,<sup>[8]</sup> and a low hydrogen content.<sup>[9]</sup> Moreover, pulsed (P)-PECVD provides an efficient energy transfer to plasma and a reduced particle size in the gas phase by controlling the duty ratio (i.e., the turn-on time). P-PECVD has been applied to the deposition of SiN films.<sup>[10-14]</sup> Several advantages of P-PECVD at room temperature in the deposition of SiN films have been reported, including less surface rough-

ness<sup>[11]</sup> and a high SiN deposition rate<sup>[12,14]</sup> at a lower duty ratio without RF-bias power in SiH<sub>4</sub>-NH<sub>3</sub> and SiH<sub>4</sub>-N<sub>2</sub> plasma. In the present study, a non-invasive ion analysis system was utilized to collect ion energy data. The data pertaining to the SiN film properties revealed useful features, such as a strong dependency of the deposition rate on ion energy or flux<sup>[12,13]</sup> or the refractive index on the ion energy flux.<sup>[8]</sup> Concerning the SiN film characteristics, the surface roughness is considerably affected by the ion energy and flux as the RF bias power varies. The relative significance of ion energy over the ion energy flux is of importance considering the formation of the surface microstructures. Unfortunately, there have been no attempts to study this issue as a function of the duty ratio. Previous work by the authors examined only the impact of the duty ratio and RF power in SiH<sub>4</sub>-NH<sub>3</sub> plasma<sup>[11]</sup> Moreover, a certain relationship between the ion energy and surface roughness can be expected. However, predicting the relationship is very difficult due to the presence of considerable unknown phenomena on film surface. One powerful means of circumventing this is to use a neural network approach. The neural network has proved its effectiveness in modeling various plasma processes.<sup>[15]</sup> No neural network models between ion energy and surface roughness have been reported.

\*Corresponding author: kbwhan@sejong.ac.kr

In this study, SiN films were deposited using P-PECVD at room temperature in SiN<sub>4</sub>-NH<sub>3</sub>-N<sub>2</sub> plasma. The surface roughness of the SiN films was investigated as a function of the duty ratio under various RF bias powers. To explore the relative influence of the ion energy, ion energy diagnostics was conducted and correlated with the surface roughness. A neural network model of the surface roughness was also constructed as a function of the ion energy variables, which were utilized to understand the parameter effects and to optimize the surface roughness.

## 2. EXPERIMENT

SiN films were deposited on p-type, single-sided polished Si wafers of the (100) orientation. The thickness and resistivity of the wafers were approximately 525 ± 25 μm and 1 Ω•cm to 30 Ω•cm, respectively. Using a P-PECVD operating at a radio frequency of 13.56 MHz at room temperature, SiN films were deposited. The equipment used to do this is identical to that in a previous work by the authors.<sup>[5]</sup> Deposition was conducted in a SiH<sub>4</sub>-NH<sub>3</sub>-N<sub>2</sub> gas mixture as a function of the bias power in the range 40W to 100 W. The source power was set to 500 W. For a given bias power, the duty ratio was varied from 30% to 90% with an increment of 20%. The flow rates of the SiH<sub>4</sub>, N<sub>2</sub>, and NH<sub>3</sub> gases were set to 8 sccm, 10 sccm, and 22 sccm, respectively. The deposition time was 5 min. The surface roughness was measured using an atomic force microscope (AFM). In order to investigate the implications of the diagnostic variables, ion energy diagnostics was conducted using a non-invasive ion energy analysis system (PLASMART<sup>TM</sup>). From the ion energy distribution functions, the main diagnostic variables were calculated. They are the E<sub>h</sub> (high ion energy), E<sub>l</sub> (low ion energy), N<sub>h</sub> (high ion energy flux) and N<sub>l</sub> (low ion energy flux). Physical definitions of these variables are available in the aforementioned study.<sup>[5]</sup> This data was used to build a neural network model of the surface roughness. Additional detail pertaining to the surface morphology can be obtained by characterizing the distribution and non-uniformity of the surface height.

## 3. RESULTS

### 3.1. Duty ratio impact on the surface roughness

Figure 1 shows the surface roughness as a function of the duty ratio at fixed bias powers. As shown in Fig. 1, the surface roughness increases and then drastically decreases as the duty ratio decreases to 100 W. Less surface roughness with as shorter duty ratio was also found in other research.<sup>[11]</sup> Ion bombardment plays a critical role in determining the surface roughness. The reduced surface roughness is caused by reduced ion bombardment stemming from the formation of a thinner plasma sheath as a result of less bias power to the plasma sheath at a shorter duty ratio. This is supported by the

E<sub>h</sub> and N<sub>h</sub> values measured at 100 W, as shown in Fig. 2. Figure 2 reveals a decrease in E<sub>h</sub> and an increase in N<sub>h</sub> with a decreasing duty ratio. In general, a decrease in the E<sub>h</sub> value produces greater surface roughness due to insufficient ion bombardment. This indicates that the surface roughness is attributed to a higher N<sub>h</sub> value. The AFM images corresponding to the duty ratios at 100 W are shown in Fig. 3. The larger surface roughness at 70% compared to that at 90%, shown in Fig. 1, is clearly ascertained by the formation of additional columns at 70%. The columns tend to decrease in relation to the number and height of the columns as the duty ratio decreases. As illustrated in Fig. 3, a very homogeneous column distribution is achieved at 30%. The surface roughness variation at 80 W is very similar to that at 100 W in the range of 50% to 90%. In contrast, the variations in the surface roughness at lower power levels of 40 W and 60 W are

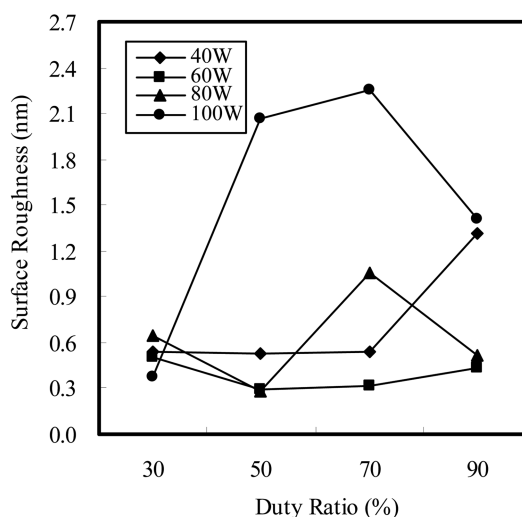


Fig. 1. Surface roughness variation as a function of duty ratio at fixed bias power.

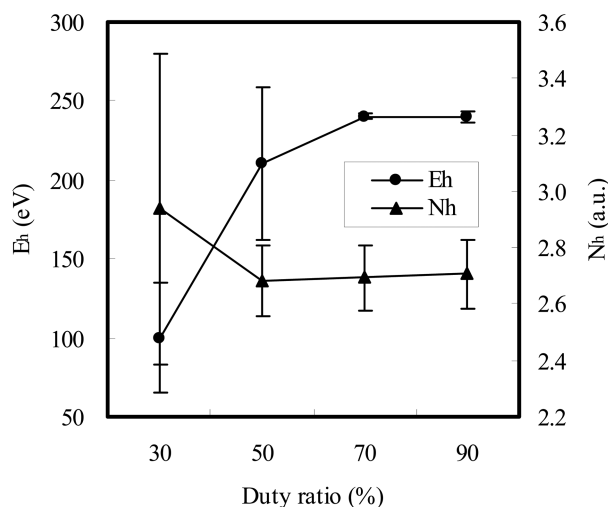


Fig. 2. Variation of E<sub>h</sub> and N<sub>h</sub> as a function of duty ratio at 100 W.

much different from those at higher powers. As supported by the AFM images shown in Fig. 4, the impact of the duty ratio

at either 40 W or 60 W is insignificant in the range of 30% to 70%. This implies that a relatively large amount of bias

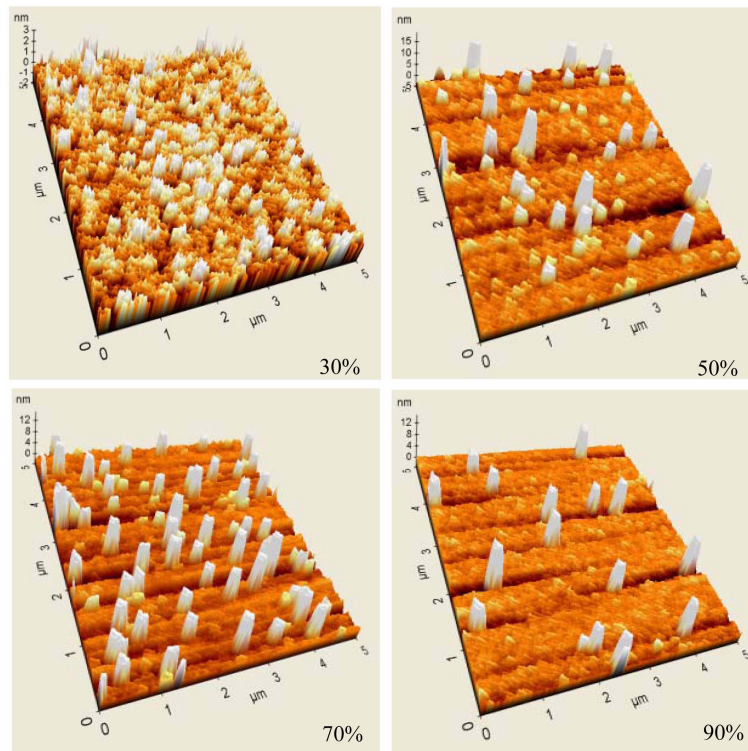


Fig. 3. AFM images as a function of duty ratio at 100 W.

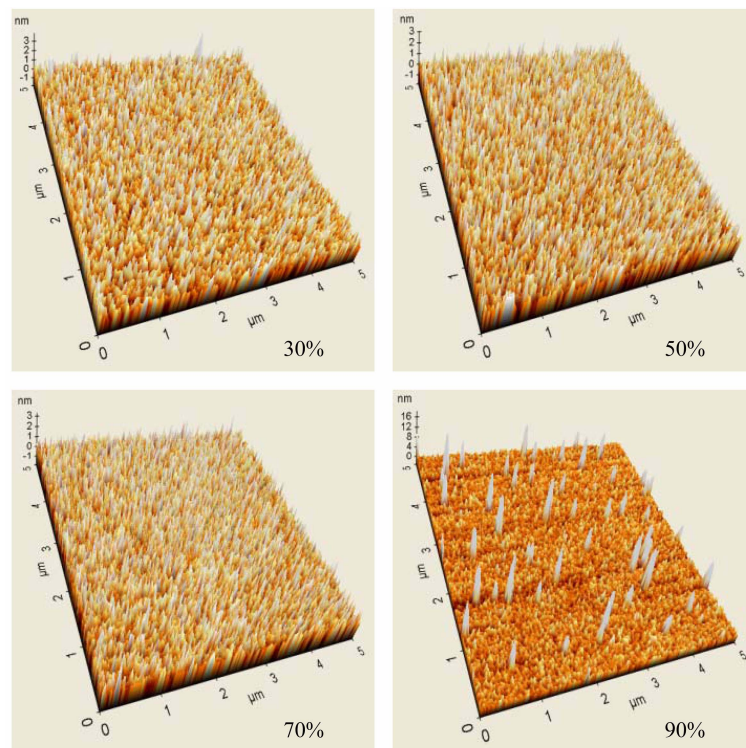


Fig. 4. AFM images as a function of duty ratio at 40 W.

power is required for the surface roughness to be controlled by the duty ratio. Figure 1 clearly shows that less surface roughness is achieved at lower duty ratios. The dominant role of  $N_h$  was already identified. It is interesting to examine the relative significance of  $N_h$  or  $N_l$ . To do this, the variation in the ratio of  $N_h$  to  $N_l$  is plotted in 5. As Fig. 5 shows, the dominance of  $N_h$  over  $N_l$  is clear at all powers except 100 W. The smaller ratio at lower duty ratios at 100 W indicates a larger  $N_l$  relative to  $N_h$  and explains the smaller surface roughness at a lower duty ratio at 100 W.

Figure 6 show the surface roughness as a function of the bias power at fixed duty ratios. As shown in Fig. 6, the smallest degree of surface roughness is obtained at 60 W at all powers except 30%. With a decrease in the power in the

range 60 to 100, the surface roughness is decreased. This is primarily due to the reduction in ion bombardment, as verified from the corresponding experimental ion energy data. Meanwhile, the ion energy flux varied slightly in the same power range. In other words, as the power varies at a different duty ratio, the surface roughness is dominated by the ion energy variation. This is different from the physical phenomenon observed earlier as the duty ratio is controlled at most duty ratios. In Fig. 6, the smallest surface roughness is obtained in all cases at 60 W. For all variations of the process parameters, the surface roughness varied between 0.285 nm and 2.249 nm. As noted in an earlier study,<sup>[11]</sup> additional details pertaining to the surface morphology is can be obtained by calculating the distribution of the pixel height as a function of the process parameters. This result is shown in Table 1, revealing that the smallest range of pixel heights as the duty ratio is controlled is between -1 and 1. To measure the non-uniformity, five samples of  $5 \mu\text{m} \times 5 \mu\text{m}$  were defined in the original AFM image. Each measured surface roughness was then used to calculate the non-uniformity, which was defined as

$$\text{Non-uniformity} = \frac{|R_c - R_a|}{R_a} \times 100 \quad (\%) \quad (1)$$

where  $R_c$  is the surface roughness measured at the center of the AFM image. Here,  $R_a$  is the average of the remaining four measurements. The results are shown in Fig. 7. Despite the complex variations with the duty ratio, the smallest degree of non-uniformity is obtained at the lowest duty ratio of 30%, except at 60 W. This implies that adopting a lower duty ratio is more likely to produce a smoother surface roughness.

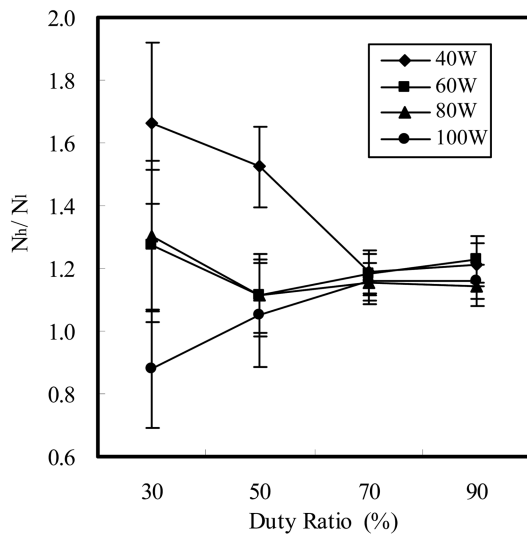


Fig. 5.  $N_h/N_l$  variation as a function of duty ratio.

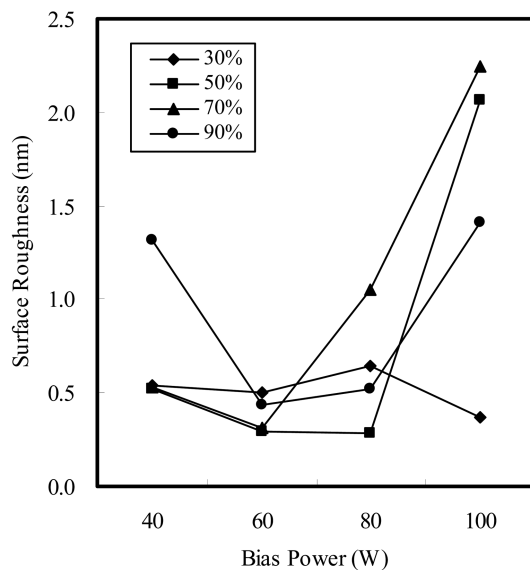
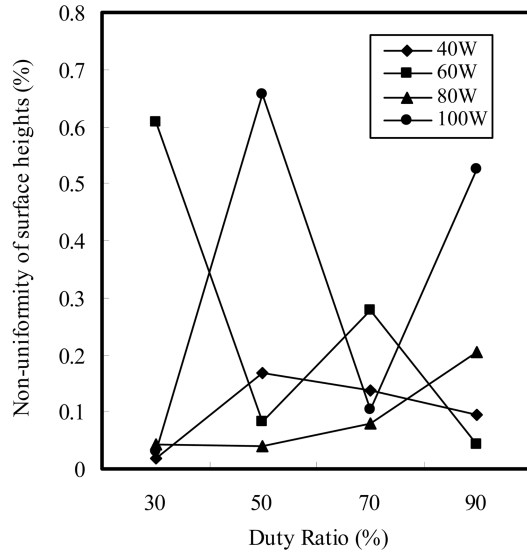


Fig. 6. Surface roughness variation as a function of bias power at fixed duty ratio.

Table 1. Distribution of surface height as a function of bias power and duty ratio

Bias Power (W)	Duty Cycle (%)	Range (nm)
40	30	-1-1
	50	-1-1
	70	-1-1
	90	-4-4
60	30	-1-1
	50	-1-1
	70	-1-1
	90	-2-2
80	30	-2-2
	50	-1-1
	70	-3-3
	90	-2-1
100	30	-1-1
	50	-5-3
	70	-4-2
	90	-1-2



**Fig. 7.** Non-uniformity of surface roughness as a function of duty ratio at fixed bias power.

### 3.2. Neural network model of surface roughness

Lastly, in order to investigate the impact of the ion energy and ion energy flux, an empirical neural network model was constructed using a generalized regression neural network (GRNN).<sup>[16]</sup> The prediction performance of the neural network model was optimized with a genetic algorithm (GA).<sup>[17]</sup> This approach has been applied to model plasma processes.<sup>[15]</sup> The training data consisted of the four diagnostic variables mentioned earlier and one output variable of the surface roughness. A typical three-layered network employing one hidden layer was employed. The learning performance of the GA-optimized neural network model as measured by  $R_2$  was about 88%. From the model, the impact of the ion energy variables can be visualized. Figure 8 shows the surface roughness as a function of the high ion energy flux ( $N_h$ ) and high ion energy ( $E_h$ ). As shown in Fig. 8, varying the  $E_h$  values slightly varies the surface roughness. In contrast, the surface roughness decreases as the  $N_h$  value decreases. Owing to the dominant role identified earlier as the duty ratio varied, the surface roughness is plotted in terms of the ion energy flux. In Fig. 9,  $N_l$  indicates the low ion energy flux. As shown in Fig. 9, decreasing  $N_h$  with a relatively high  $N_l$  value tends to decrease the surface roughness. The smallest surface roughness appears to have been obtained with an  $N_l$  value between 3.0 and 3.5 with the lowest  $N_h$  value. A further decrease in the surface roughness can be expected by decreasing the  $N_h$  more given a set  $N_l$ .

## 4. CONCLUSION

Using pulsed PECVD, silicon nitride films were deposited in  $\text{SiH}_4\text{-NH}_3\text{-N}_2$  plasma at room temperature. Ion energy

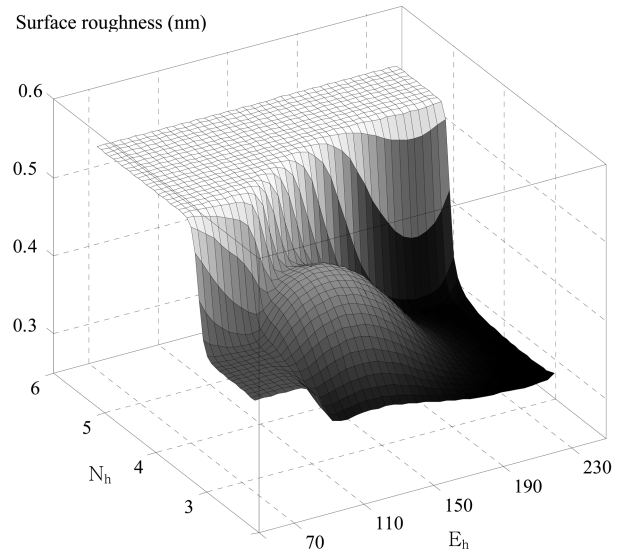


**Fig. 8.** Surface roughness model as a function of  $N_h$  and  $E_h$ .

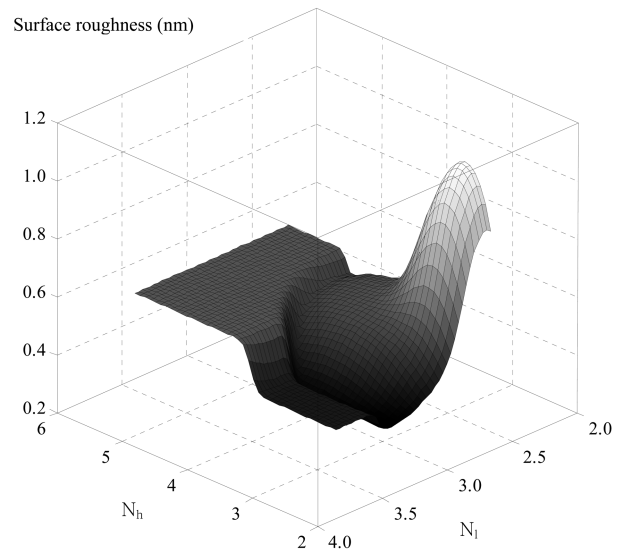


**Fig. 9.** Surface roughness model as a function of  $N_h$  and  $E_l$ .

diagnostic data were correlated with the SiN surface morphology. In addition, a neural network model was built to facilitate an understanding of the impact of the diagnostic variables on the surface morphology. The surface morphology was detailed in terms of several features. One important finding is that adopting a smaller duty ratio is advantageous when seeking to optimize the mean surface roughness and obtain non-uniformity of the film surface. It was also noted that the smallest degree of surface roughness is strongly correlated with the  $N_h$  value as the duty ratio varied. This indicates the significance of controlling the  $N_h$  values during optimization of the surface roughness. This was supported further by the neural network model. The model predicted

that high ion energy flux plays a more important role in optimizing the surface roughness.

## ACKNOWLEDGMENT

This research was supported by Basic Science Research Program through the National Research Foundation of Korea (NRF) funded by the Ministry of Education, Science and Technology (2009-0087476).

## REFERENCES

1. S. Bae, D. G. Farber, and S. J. Fonash, *Solid State Electron.* **44**, 1355 (2000).
2. G. Suchaneck, V. Norkus, and G. Gerlach, *Surf. Coat. Technol.* **142**, 808 (2001).
3. J.-D. Gu and P.-Li Chen, *Thin Solid Films* **498**, 2 (2006).
4. T. T. T. Pham, J. H. Lee, Y. S. Kim and G. Y. Yeom, *Surf. Coat. Technol.* **202**, 5617 (2008).
5. B. Kim and S. Kim, *Met. Mater. Int.* **14**, 637 (2008).
6. R. Wolf, K. Wandel, and B. Gruska, *Surf. Coat. Technol.* **142**, 786 (2001).
7. M. Medjdoub, J. L. Courant, H. Maher, and G. Post, *Mater. Sci. Engr. B* **80**, 252 (2002).
8. S. Kim and B. Kim, *Met. Mater. Int.* **15**, 881 (2009).
9. H. Zhou, K. Elgaid, C. Wilkinson, and I. Thayne, *J. J. Appl. Phys.* **45**, 8388 (2006).
10. R. Vernhes, O. Zabeida, J. E. Klemberg-Sapieha, and L. Martinu, *J. Appl. Phys.* **100**, 063308 (2006).
11. B. Kim, S. Kim, Y. H. Seo, S. J. Kim, and S. C. Jung, *J. Nano Sci. Technol.* (2008).
12. B. Kim and S. Kim, *Thin Solid Films* **517**, 4090 (2009).
13. S. Kim and B. Kim, *Curr. Appl. Phys.*, doi:10.1016/j.cap.2010.02.033 (2010).
14. H. Lee, B. Kim, and S. Kwon, *Curr. Appl. Phys.*, doi:10.1016/j.cap.2009.12.023 (2010).
15. B. Kim, M. Kwon, and S. Kwon, *Microelectron. Eng.* **86**, 63 (2009).
16. D. F. Specht, *IEEE T. Neural Networ.* **2**, 568 (1991).
17. D. E. Goldberg, *Genetic Algorithms in Search, Optimization & Machine learning*, Addison Wesley, Reading, MA (1989).